International Journal of Engineering Research-Online
*A Peer Reviewed International Journal*
Articles available online http://www.ijoer.in; editorijoer@gmail.com

Vol.6., Issue.5, 2018
Sept-Oct.,

RESEARCH ARTICLE

ISSN: 2321-7758

# Effects of Deposition Time on Thin Films of PbS Produced by Using Chemical Bath Deposition Method

**Ayça KIYAK YILDIRIM**
Department of Motor Vehicles and Transportation Technologies, BilecikŞeyhEdebali University
BilecikŞeyhEdebali University,11210Bilecik/Turkey &0228 214 1111
ayca.kiyak@bilecik.edu.tr

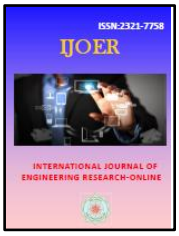


**ABSTRACT**
Chemical bath deposition (CBD) method was used to deposit thin films of PbS. In the experiments, PbS was obtained at five rent deposition times which are 15, 25, 35, 45 and 55 minutes. The effects of deposition time were investigated in detail. The structural properties of the PbS films were examined by using X-ray diffractometer (XRD). According to the XRD, it was found that when deposition time was increased, the intensity of the peaks increased and the crystallization of PbS thin films were improved. All PbS films thickness increased as depending on the deposition time increased. Besides, crystallite sizes, lattice constants, average stresses, micro strains and dislocation densities were obtained from the XRD results. According to them, the micro strain and average stress of the film significantly decreased as depending on the deposition time increased. Surface properties of the PbS thin films were researched by using scanning electron microscope (SEM). The SEM images revealed that when deposition time was increased, pinholes and voids formations were less appeared on the film surface.

## 1. INTRODUCTION

Lead sulfide (PbS) is a semiconducting chalcogenide and belongs to groups IV–VI compound semiconductor with direct narrow band gap energy of 0.41 eV (at 300 K) PbS has a cubic structure and a relatively large exciton Bohr radius (18 nm) [1].

For the past few years, the properties of PbS film for the research on the growth of nano particle PbS films has increased for its technological various nanodevice applications have been studied such as [2], infrared detection [3],[4], photosensitive resistance, light-emitting diodes, optoelectronic devices, humidity and temperature sensors, widely used in IR detectors. Owing to their suitable bandgaps, PbS thin films using solar control coatings [5], [6]. The possibility of using very thin (20–60 nm) chemically deposited PbS films as solar control coatings have been discussed by many workers [7],[8]. Polycrystalline PbS films can be obtained by several methods such as spray pyrolysis [9], successive ionic layer adsorption and reaction [10], thermal evaporation [11], solid-vapor deposition [12], galvanic method [13], atomic layer deposition [14], pulse electrodeposition [15],[16], electrodeposition [17]-[21] microwave heating [22], and chemical bath deposition (CBD) [23]-[26]. Among these methods, CBD is more widely utilized due to its low cost, not require sophisticated and expensive İnstruments [2], [27], easy to handle, the quality of the films, and convenience for large area deposition and on various substrates [28], [29].

Many researchers have reported properties of chemically deposited PbS thin films. The method of chemical bath deposition (CBD) is based on successive adsorption and reaction of species on the substrate surface from aqueous solutions [27],[2].

The mechanisms of reactions for PbS precipitation that take place during the production of PbS with the chemical bath deposition is as follows [23]:

$$Pb(NO_3)_2 + 2NaOH \rightarrow Pb(OH)_2 + 2NaNO_3 \quad (1)$$

$$Pb(OH)_2 + 2NaOH \rightarrow Na_2[Pb(OH)_4] \quad (2)$$

$$[Pb(OH)_4]^{2-} \rightarrow Pb^{2+} + 4OH^- \quad (3)$$

$$CS(NH_2)_2 + OH^- \rightarrow CH_2N_2 + H_2O + HS^- \quad (4)$$

$$HS^- + OH^- \rightarrow H_2O + S^{2-} \quad (5)$$

$$Pb^{2+} + S^{2-} \rightarrow PbS \quad (6)$$

## II. PROCEDURE

### *A. Thin films deposition*

The glass slides of dimension 4 cm x 2.5 cm x 2 mm were cleaned as the clean lines of the substrate has a direct bearing on the adherence of the film. The deposition solution was prepared in a 100 ml deionize water containing with 0.009 M of lead nitrate [Pb $(NO_3)_2$]), 0.051M thiourea $(CS(NH_2)_2)$ and 0.30 M of Thiourea $[SC(NH_2)_2]$. The alkalinity is set using, sodium hydroxide (NaOH) of 0.64 M. Deposition solutions were mixed at 600 rpm. All solution was prepared at 11 pH. The glass substrates and deposition bath were cleaned with 5% (w/w) hydrochloric acid and after than were washed with deionized water. Cleaned glass substrates were immersed vertically into the deposition bath. The PbS films were deposited at various time from 15 to 55 minutes. The temperature of the solution in the bath was maintained at room temperature (300 K). After the deposition the substrates were taken out of the deposition bath and rinsed thoroughly with deionized water and dried in air. Mirror-like gray thin film surfaces were obtained after removal of one side of the glass slide using cotton with HCL. The deposited films were found to be well adherent, uniform, dark brownish black in color.

### *B. Characterizations of thin films*

The synthesized PbS thin films were characterized for their structural and morphological properties. Film thickness was measured using an optical reflectometer (Filmetrics F20) and gravimetric method was used to calculate film thicknesses.

The X-ray diffraction spectroscopy (XRD) analysis was used to a PA Nalytical Empyrean XRD in the range of 20–80 with Cu Kα of 1.5410 A°. The surface morphology of the prepared samples was investigated by using a Zeiss SUPRA 40VP scanning electron microscope (SEM).

## III. RESULTS

### *A. Structural studies of PbS thin films*

The properties of the films examined by XRD technique such as crystal structure, crystalite size, preferential orientation, strain and stress acting on the unit surface have been determined. The diffraction peaks observed at diffraction angles 2θ of 25.9 °; 30 °; 43 °; 50.9 °; 53.4 ° and 62.5 ° correspond to the (111), (002), (022), (113) and (222) planes of the cubic PbS type structure. E1, E2, E3, E4 and E5 are confirmed by the ASTM number (98-060-0243),(98-003-8293), (98-006-3095), (98-006-2193) and (98-006-2193), respectively. It has been observed that the intensity of the peaks increased and the crystallization of PbS thin films were improved with increasing deposition times. XRD analyzes of PbS thin films produced in E1, E2, E3, E4 and E5 are given in Figure 1 and they revealed that all films formed in cubic galena structure.

Film thicknesses were calculated by using gravimetric method and results were given in Table 1. While the thicknesses of the PbS films were being varied between 526 nm and 698 nm. This result showed that deposition time did affect the film thicknesses. The PbS film thickness increased as depending on the deposition time increased.

The texture coefficients, given in Equation 7 [30], of the films were employed to determination of preferred orientation.

$$TC = \frac{I_{(hkl)}/I_{0(hkl)}}{\frac{1}{N}\sum_N (\frac{I_{(hkl)}}{I_{0(hkl)}})} \quad (7)$$

where I (hkl) is the measured relative intensity of a plane (hkl), $I_0$(hkl) is the standard intensity of the plane (hkl) given in ASTM card. The calculated texture coefficients were given in Table 1. It has been determined that all films have 3 texture coefficient values larger than 1 belonging to different planes. The preferred orientation for all films produced is thought to be random. According to the texture coefficients although the films produced at 35, 45 and 55 minutes, the peak intensity of (111) plane of the film was higher than that of the (002) plane. This result is an expected result according to the previousstudy in the literature, it was observed in the experiment in which no inhibitor was used in the deposition solution that the lead concentration at room

temperature was almost complete in 50 minutes [23]. Due to this reason, the peak intensity of (111) plane of the film cannot be expected to shift towards the (002) plane.

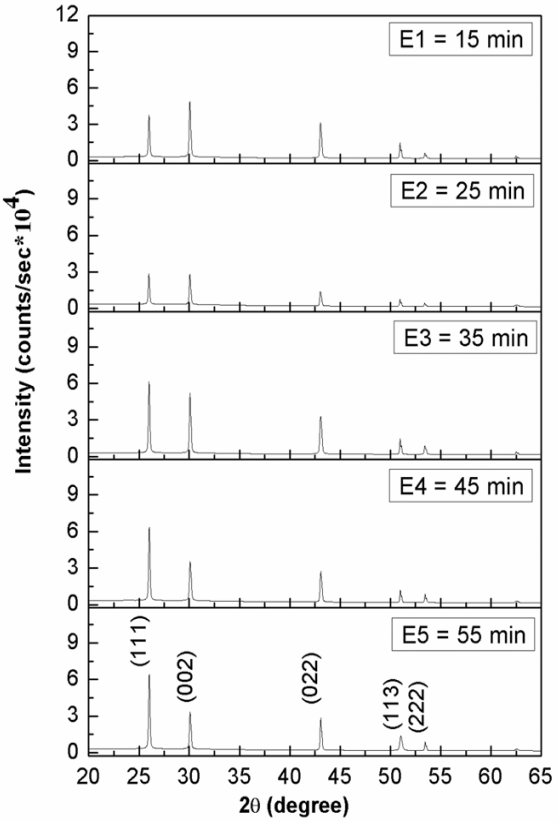


**Fig.1**X-ray diffractograms of PbS thin films according to deposition time

The average crystallite sizes of samples were estimated Debye Scherrer equation given in Equation 8.

$$cs = \frac{0.089*180*\lambda}{314*\beta*\cos\theta_C} nm \quad (8)$$

where$\lambda$ was the wavelength of X-ray radiation (1.54056 Å), $\beta$was the full width half maximum, $2\theta_C$ was the peak centre, $\beta$and $2\theta_C$were calculated by fitting the XRD peak profile [31]. The estimated crystallite sizes of the films were given in Table2. When Table2 is examined, it can be seen that crystallite size varies from 30 nm to 93nm. The lattice constant of the cubic rock salt structure is given as follows by [32].

$$a = d\sqrt{(h^2 + k^2 + l^2)} \quad (9)$$

where h, k and l are the Miller indices and d is the interplanar distance. Furthermore, the micro strain and average stress were calculated by using Equation 10 and 11 respectively and given in Table2.

$$\varepsilon = (a_0 - a)/a_0 \quad (10)$$

$$S = \varepsilon Y/(2\sigma) \quad (11)$$

Where $a_0$ and a are lattice parameter of the bulk sample and the corrected value of lattice parameter of thin film samples respectively. The σ and Y are the Poisson's ratio and Young's modulus of the bulk crystal respectively. For PbS the value of Y is 70.2 GPa and σ is 0.28.

**Table 1.**The intensity, texture coefficient and film thickness of the PbS thin films produced at 15, 25, 35, 45 and 55 minutes

| EXPERIMENT | 2θ | INTENSITY (COUNT/ SECONDS) | $I/I_o$ | TC | (hkl) | FILM THICKNESS (nm) |
|---|---|---|---|---|---|---|
| E1 | 25,972 | 37605,30 | 71,95 | 1,691 | (111) | 526 |
| | 30,053 | 48873,16 | 100 | 2,350 | (002) | |
| | 43,045 | 31344,85 | 69,05 | 1,623 | (022) | |
| | 50,960 | 14553,44 | 33,08 | 0,777 | (113) | |
| | 53,432 | 6151,78 | 11,4 | 0,268 | (222) | |
| | 62,498 | 3719,75 | 5,61 | 0,132 | (004) | |
| | 68,892 | 4030,63 | 6,78 | 0,159 | (133) | |
| E2 | 25,960 | 27611,30 | 96,06 | 2,222 | (111) | 547 |
| | 30,057 | 27970,74 | 100 | 2,313 | (002) | |
| | 43,037 | 13897,94 | 53,68 | 1,242 | (022) | |
| | 50,954 | 7480,71 | 27,96 | 0,647 | (113) | |
| | 53,405 | 4311,75 | 13,29 | 0,307 | (222) | |
| | 62,510 | 2979,58 | 5,26 | 0,122 | (004) | |
| | 68,877 | 2797,06 | 6,39 | 0,148 | (133) | |
| E3 | 25,978 | 61523,92 | 100 | 2,314 | (111) | 596 |
| | 30,071 | 52205,38 | 89,05 | 2,060 | (002) | |
| | 43,053 | 32821,82 | 58,59 | 1,356 | (022) | |
| | 50,969 | 14571,67 | 27,93 | 0,646 | (113) | |
| | 53,422 | 8929,49 | 14,93 | 0,345 | (222) | |
| | 62,521 | 4060,85 | 5,38 | 0,124 | (004) | |
| | 68,902 | 4332,48 | 6,65 | 0,154 | (133) | |
| E4 | 25,998 | 61092,01 | 100 | 2,889 | (111) | 647 |
| | 30,084 | 33366,29 | 52,03 | 1,503 | (002) | |
| | 43,071 | 27386,65 | 47,51 | 1,372 | (022) | |
| | 50,989 | 11833,02 | 20,68 | 0,597 | (113) | |
| | 53,446 | 8494,17 | 14,1 | 0,407 | (222) | |
| | 62,531 | 3074,51 | 2,78 | 0,080 | (004) | |
| | 68,928 | 4003,78 | 5,22 | 0,151 | (133) | |
| E5 | 25,996 | 62251,18 | 100 | 2,831 | (111) | 698 |
| | 30,080 | 32348,27 | 51,87 | 1,469 | (002) | |
| | 43,070 | 28536,40 | 51,39 | 1,455 | (022) | |
| | 51,017 | 12709,31 | 20,52 | 0,581 | (113) | |
| | 53,449 | 9042,65 | 14,94 | 0,423 | (222) | |
| | 62,523 | 2999,58 | 2,62 | 0,074 | (004) | |
| | 68,919 | 4294,17 | 5,88 | 0,166 | (133) | |

**Table 2.**The crystalite size, dislocation densities, lattice parameter, micro strain values, and average stress values of the PbS thin films produced at 15, 25, 35, 45 and 55 minutes

| EXPERIMENT | 2θ | CRYSTALITE SIZE(nm) | LATICE PARAMETERa (VERIFIED) (Å) | MICRO STRAIN $*10^{-3}$ | DISLOCATION DENSITY (lines/m$^2$)$*10^{14}$ | AVERAGE STRESS ($10^8$N/m$^2$) |
|---|---|---|---|---|---|---|
| E1 | 25,972 | 63 | 5,9424 | 1,07 | 2,52 | 1,34 |
| | 30,053 | 64 | 5,9472 | 1,88 | 2,47 | 2,36 |
| | 43,045 | 66 | 5,9437 | 1,30 | 2,30 | 1,63 |
| | 50,960 | 85 | 5,9436 | 1,27 | 1,38 | 1,60 |
| | 53,432 | 86 | 5,9404 | 0,74 | 1,35 | 0,93 |
| | 62,498 | 90 | 5,9445 | 1,44 | 1,24 | 1,80 |
| | 68,892 | 93 | 5,9411 | 0,86 | 1,15 | 1,08 |
| E2 | 25,960 | 63 | 5,9450 | 1,51 | 2,52 | 1,89 |
| | 30,057 | 64 | 5,9463 | 1,74 | 2,47 | 2,18 |
| | 43,037 | 66 | 5,9447 | 1,47 | 2,30 | 1,84 |
| | 50,954 | 85 | 5,9443 | 1,39 | 1,38 | 1,74 |
| | 53,405 | 86 | 5,9432 | 1,21 | 1,35 | 1,52 |
| | 62,510 | 30 | 5,9435 | 1,26 | 1,24 | 1,58 |
| | 68,877 | 74 | 5,9422 | 1,04 | 10,4 | 1,31 |
| E3 | 25,978 | 63 | 5,9400 | 0,67 | 2,52 | 0,85 |
| | 30,071 | 64 | 5,9436 | 1,27 | 2,47 | 1,60 |
| | 43,053 | 55 | 5,9426 | 1,11 | 2,30 | 1,40 |
| | 50,969 | 85 | 5,9426 | 1,11 | 1,38 | 1,39 |
| | 53,422 | 69 | 5,9414 | 0,91 | 2,17 | 1,14 |
| | 62,521 | 90 | 5,9425 | 1,09 | 1,24 | 1,37 |
| | 68,902 | 93 | 5,9403 | 7,26 | 1,16 | 0,91 |
| E4 | 25,998 | 63 | 5,9365 | 0,09 | 2,52 | 0,11 |
| | 30,084 | 53 | 5,9411 | 0,86 | 3,56 | 1,08 |
| | 43,071 | 66 | 5,9403 | 0,72 | 2,30 | 0,90 |
| | 50,989 | 85 | 5,9404 | 0,75 | 1,38 | 0,94 |
| | 53,446 | 86 | 5,9390 | 0,50 | 1,35 | 0,63 |
| | 62,531 | 45 | 5,9416 | 0,95 | 4,96 | 1,19 |
| | 68,928 | 74 | 5,9383 | 0,40 | 1,80 | 0,50 |
| E5 | 25,996 | 63 | 5,9368 | 0,14 | 2,52 | 0,17 |
| | 30,080 | 64 | 5,9419 | 0,10 | 2,47 | 1,24 |
| | 43,070 | 83 | 5,9404 | 0,74 | 1,47 | 0,93 |
| | 51,017 | 43 | 5,9374 | 0,23 | 5,53 | 0,29 |
| | 53,449 | 86 | 5,9386 | 0,45 | 1,35 | 0,56 |
| | 62,523 | 45 | 5,9424 | 1,07 | 4,96 | 1,34 |
| | 68,919 | 93 | 5,9390 | 0,51 | 1,15 | 0,63 |

The corrected values are estimated from the Nelson–Riley plots given in Fig.2, Fig.3, Fig.4 Fig.5and Fig.6. The lattice parameters calculated from the peak positions of individual reflections are plotted against $F(\theta) = (cos^2\theta/2) * (\frac{1}{sin^2\theta} + \frac{1}{\theta})$ and the intercept of the linear plot at $(cos^2\theta/2) * (\frac{1}{sin^2\theta} + \frac{1}{\theta}) = 0$ at gives the corrected lattice constant [33]. Deviation of the calculated lattice parameter (a) from the strain face bulk sample ($a_0$ = 5.936 nm) indicates that the as obtained films were under strain [33].

Dislocation density can be derived from the crystallite size as given in Equation 12 presented in Table 2[34]

$$\delta = \frac{1}{(cs)^2} \quad (12)$$

According to Table 2, the micro strain and average stress of the film significantly decreased as depending on the deposition time increased.

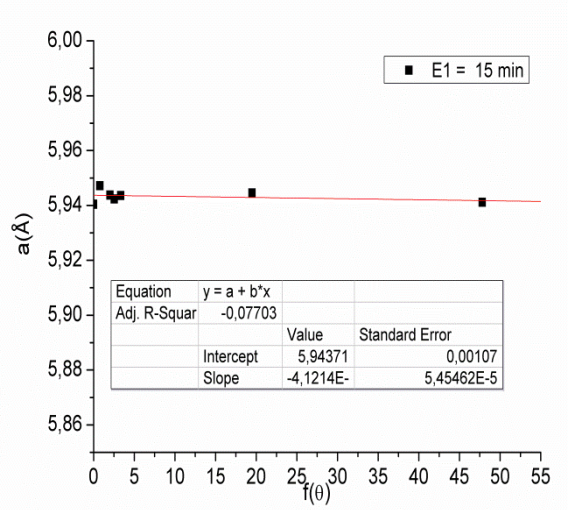


**Fig.2** Nelson–Riley plots of PbSthin films obtained at 15 minute

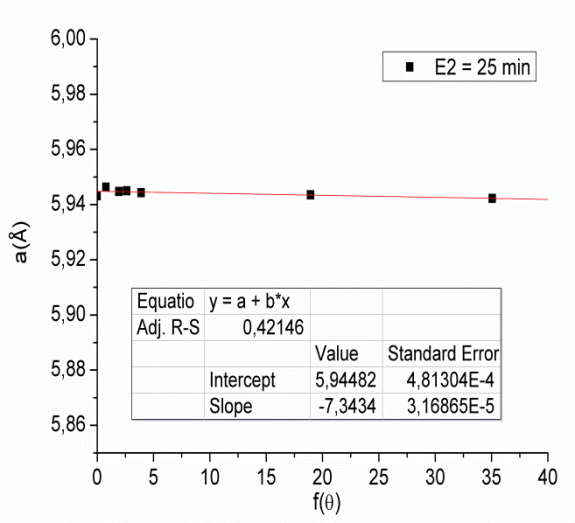


**Fig.3** Nelson–Riley plots of PbS thin films obtained at 25 minute

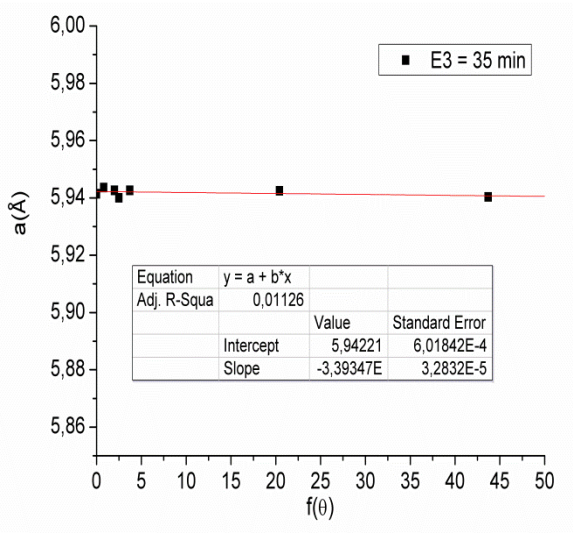


**Fig.4** Nelson–Riley plots of PbS thin films obtained at 35 minute

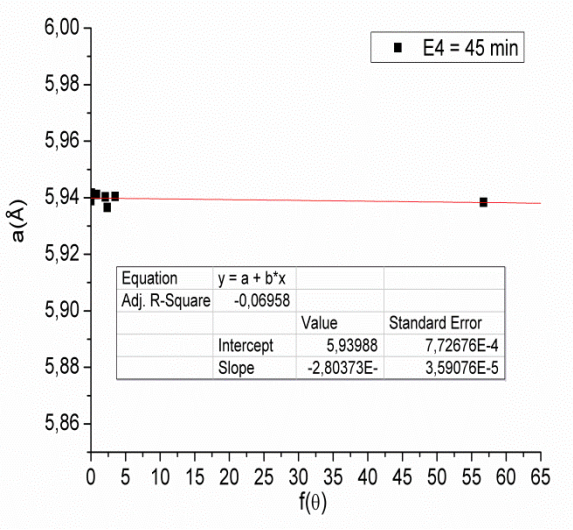


**Fig.5**Nelson–Riley plots of PbS thin films obtained at 45 minute

**E5 = 55 MINUTE**

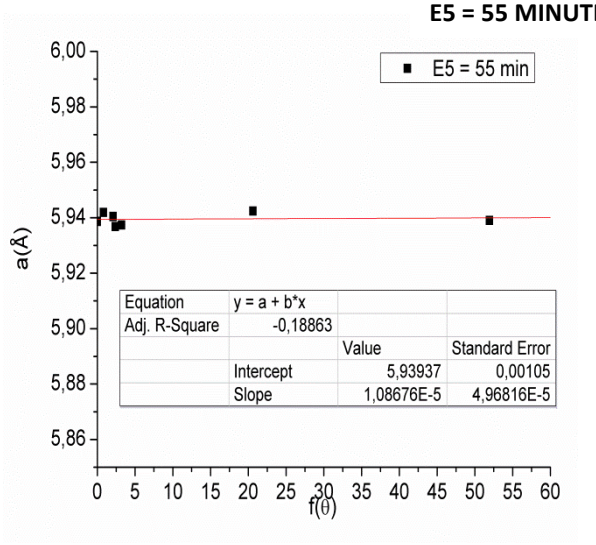


**Fig.6** Nelson–Riley plots of PbS thin films obtained at 55 minute

*B. Surfaces of PbS thin films*

Typical 100 times magnified SEM images were given in Fig.7 and Fig.8. There are plenty of voids and pinholes on the surface of the films obtained with 15, 25 and 35 minutes given in Fig.7a, Fig.7b and Fig.7c respectively. It was showed in a previous study [35] that pinholes and voids could be seenPbS films which obtained at 30 minute.

It is thought that increasing deposition time decreased pinholes and voids formations as given in Figure 8a, and 8b. Besides, these surfaces are shown nearly compact and nearly smooth.

The 30000 times magnified surface images were given in Fig.9 and Fig.10.The films obtained with 35, 45 and 55 minute given in Fig.9c, Fig.10a and Fig.10b respectively. These surfaces are seen typical morphology of PbS films. The sizes of the polymorphic particles vary between 200 nm and 1000nm. It is noteworthy that there are not pinholes and voids on these surfaces. This result showed that relatively high SEM images can be fallacious for people.

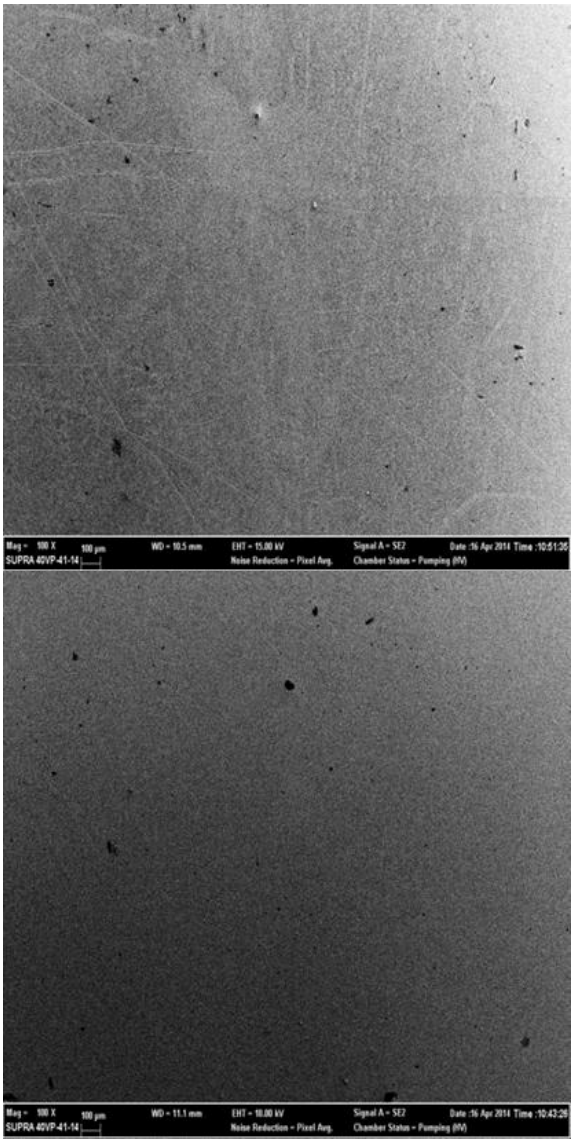

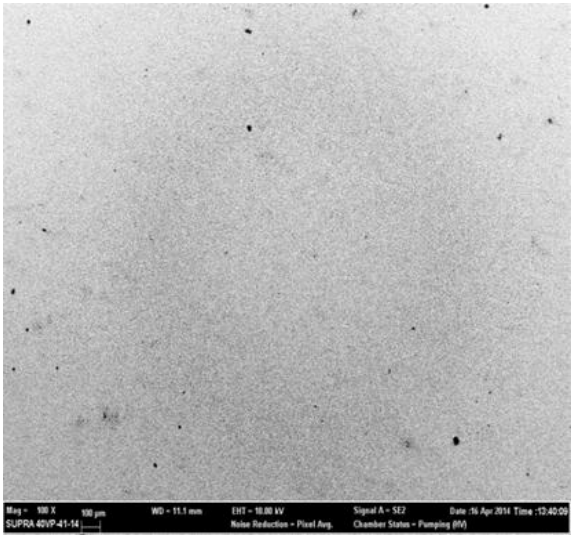

**Fig.7**SEM images of the PbS films obtained at a)15 b) 25 c) 35 minutes magnified 100 times.

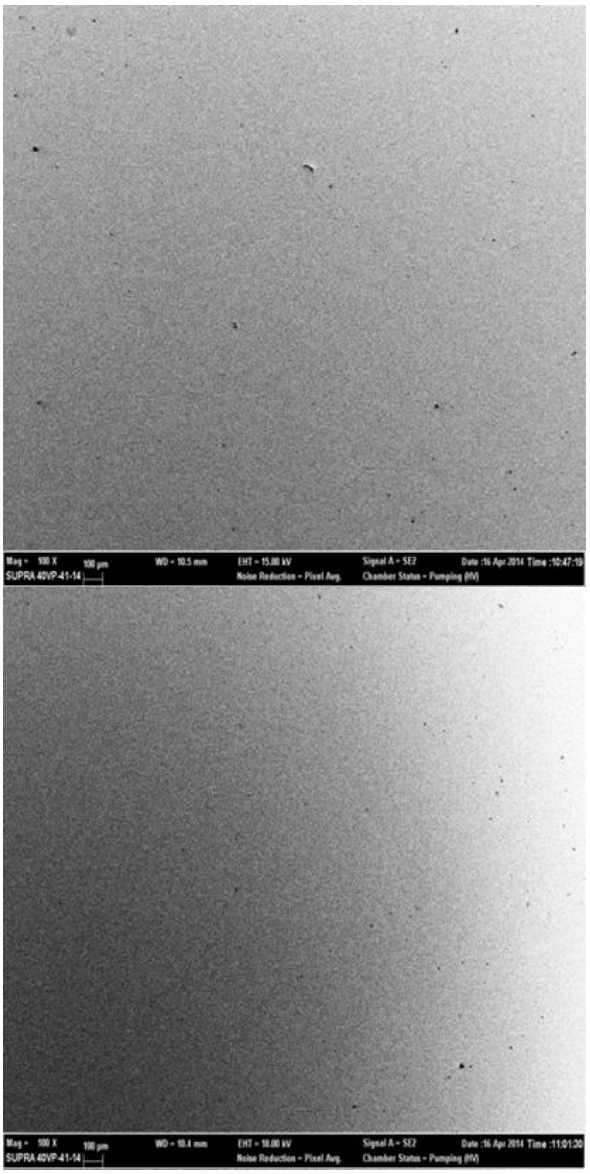

**Fig.8** SEM images of the PbS films obtained at a)45 b) 55 minutesmagnified100 times

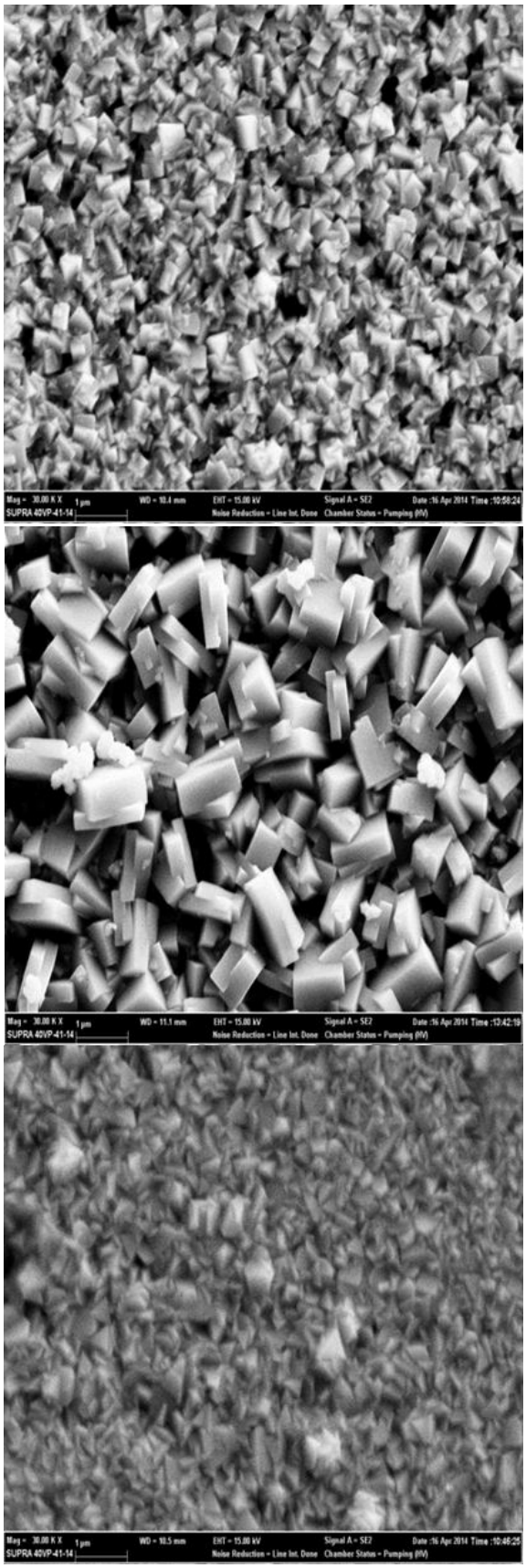

**Fig.9** SEM images of the PbS films obtained at a)15 b) 25 c)35 minutes magnified 30000 times.

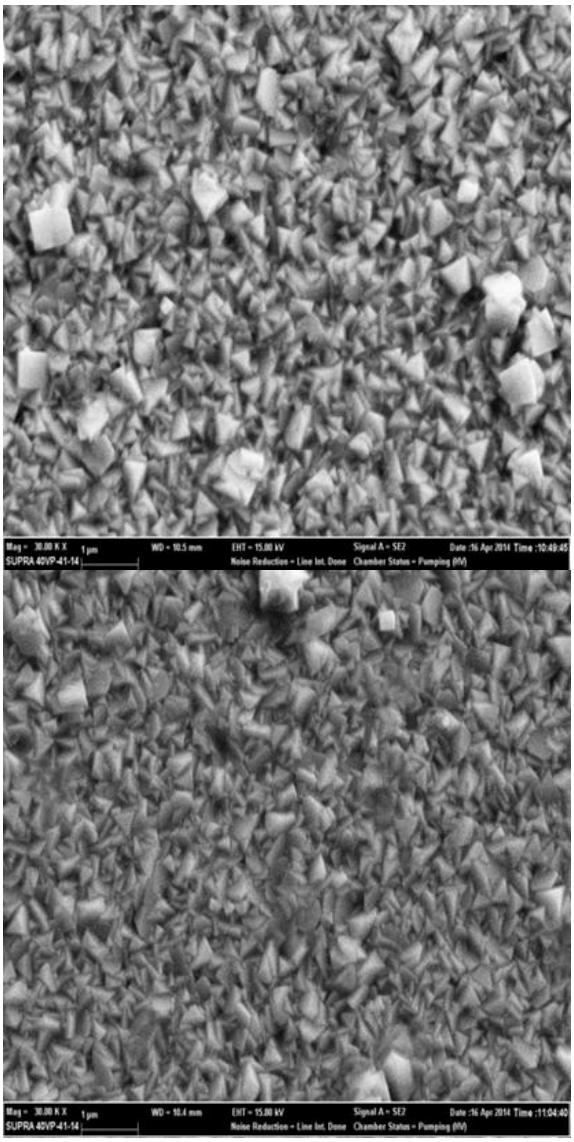

**Fig.10** SEM images of the PbS films obtained at a)45 b) 55 minutesmagnified30000times

## IV. CONCLUSIONS

In this study, PbS thin films were produced by chemical bath deposition. Five different deposition times were applied in the experiments. XRD data showed that the intensity of the peaks increased and the crystallization of PbS thin films were improved with increasing deposition times.All PbSfilms formed in cubic structure and their thickness increased as depending on the deposition time increased. Besides, the films produced at 15 and 25 minutes, the peak intensity of(002) plane of the film was higher than that of the (111) plane. Although the films produced at 35, 45 and 55 minutes, the peak intensity of (111) plane of the film was higher than that of the (002) plane. This result is

an expected result because of the previous study in the literature; it was observed that the lead concentration at room temperature was almost complete in 50 minutes [23]. Thence, the peak intensity of (111) plane of the film cannot be anticipated to shift towards the (002) plane.

Dislocation densities, micro strain, and average stress values of all films were calculated. The micro strain and average stress of the film significantly decreased as depending on the deposition time increased. Among all films, any film had not negative average stress and micro strain values. It is clearly understood that no negative strain indicates no compressive strain present in the synthesized PbS thin films [36].

The surface morphologies were investigated by using a SEM and the SEM images revealed that when deposition time was increased, pinholes and voids formations wereless appeared on the film surface. The 30000 times magnified surface images of the films obtained with 35, 45 and 55 minute are seen typical polymorphic morphology. It is noteworthy that there are not pinholes and voids on these surfaces. Due to this result, relatively high SEM images can be deceptive for people.

**REFERENCES**

[1]. Joshi, R., Kanjilal, A. and Sehgal, H. (2004). Solution grown PbS nanoparticle films. Applied Surface Science, 221(1-4), pp.43-47.

[2]. Saravana Kumaran, T. and ParveenBanu, S. (2013). investigation on structural and optical properties of chemically deposited PbS thin films. International Journal of Recent Scientific Research Research, 4(1), pp.1685-1687.

[3]. Moreno-García, H., Nair, M. and Nair, P. (2011). Chemically deposited lead sulfide and bismuth sulfide thin films and $Bi_2S_3$/PbS solar cells. Thin Solid Films, 519(7), pp.2287-2295.

[4]. Seghaier, S., Kamoun, N., Brini, R. and Amara, A. (2006). Structural and optical properties of PbS thin films deposited by chemical bath deposition. Materials Chemistry and Physics, 97(1), pp.71-80.

[5]. Osherov, A., Makai, J., Balazs, J., Horvath, Z., Gutman, N., Sa'ar, A. and Golan, Y. (2010). Tunability of the optical band edge in thin PbS films chemically deposited on GaAs(100). Journal of Physics: Condensed Matter, 22(26), p.262002.

[6]. Nair, P., Garcia, V., Hernandez, A. and Nair, M. (1991). Photoaccelerated chemical deposition of PbS thin films: novel applications in decorative coatings and imaging techniques. Journal of Physics D: Applied Physics, 24(8), pp.1466-1472.

[7]. Espevik, S., Wu, C. and Bube, R. (1971). Mechanism of Photoconductivity in Chemically Deposited Lead Sulfide Layers. Journal of Applied Physics, 42(9), pp.3513-3529.

[8]. Nair, P., Nair, M., Fernandez, A. and Ocampo, M. (1989). Prospects of chemically deposited metal chalcogenide thin films for solar control applications. Journal of Physics D: Applied Physics, 22(6), pp.829-836.

[9]. Thiagarajan, R., MahaboobBeevi, M., Anusuya, M. and Ramesh, T. (2012). Influence of reactant concentration on nano crystalline PbS thin films prepared by Chemical Spray Pyrolysis. Optoelectronics and Advanced Materials – Rapid Communications, 6(1), pp.132-135.

[10]. Kanniainen, T., Lindroos, S., Resch, R., Leskelä, M., Friedbacher, G. and Grasserbauer, M. (2000). Structural and topographical studies of SILAR-grown highly oriented PbS thin films. Materials Research Bulletin, 35(7), pp.1045-1051..

[11]. Ibrahim, A. (2009). Structure and electronic properties of evaporated thin films of lead sulfide. Defect and Diffusion Forum, 294, pp.85-92.

[12]. Obaid, A., Mahdi, M. and Zainuriah, H. (2012). Growth of nanocrystallinePbSthin films by solid-vapor deposition. Advanced Materials Research, 620, pp.1-6.

[13]. Mondal, A. and Mukherjee, N. (2006). Cubic PbS thin films on TCO glass substrate by

galvanic technique. Materials Letters, 60(21-22), pp.2672-2674.

[14]. Dasgupta, N., Lee, W. and Prinz, F. (2009). Atomic layer deposition of lead sulfide thin films for quantum confinement. Chemistry of Materials, 21(17), pp.3973-3978.

[15]. Mathews, N., Ángeles–Chávez, C., Cortés-Jácome, M. and Toledo Antonio, J. (2013). Physical properties of pulse electrodeposited lead sulfide thin films. ElectrochimicaActa, 99, pp.76-84.

[16]. Thirumoorthy, P. and Murali, K. (2010). Characteristics of pulse electrodeposited PbS thin films. Journal of Materials Science: Materials in Electronics, 22(1), pp.72-76.

[17]. KıyakYıldırım, A. and Altıokka, B. (2017). An investigation of effects of bath temperature on CdO films prepared by electrodeposition. Applied Nanoscience. doi: 10.1007/s13204-017-0591-x

[18]. KıyakYıldırım, A. and Altıokka, B. (2017). Effects of concentration on CdOfilms grown by electrodeposition. Applied Nanoscience. 7:131–135. doi:10.1007/s13204-017-0552-4

[19]. Altıokka, B. and KıyakYıldırım, A. (2015). Effects of external alternating magnetic field on ZnO films obtained by electrodeposition. Arabian Journal for Science Engineering. doi: 10.1007/s13369-015-1980-7

[20]. Altıokka, B. and KıyakYıldırım, A. (2018). Effects of pH on CdO films deposited onto ITO coatedglass substrates by electrodeposition. Int. J. Surface Science and Engineering, 12(1), pp.13-22.

[21]. Altıokka, B. and KıyakYıldırım, A. (2018). Electrodeposition of CdS Thin Films at Various pH Values. Journal of the Korean Physical Society, 72(6), pp.687-691.

[22]. Zhao, Y., Liao, X., Hong, J. and Zhu, J. (2004). Synthesis of lead sulfide nanocrystals via microwave and sonochemical methods. Materials Chemistry and Physics, 87(1), pp.149-153.

[23]. Altıokka, B., Baykul, M., Altıokka, M., 2013. Some physical effects of reaction rate on PbS thin films obtained by chemical bath deposition. Journal of Crystal Growth, 384, pp.50-54.

[24]. Altıokka, B., 2015. Effects of Inhibitor on PbS Thin Films Obtained by Chemical Bath Deposition. Arabian Journal for Science and Engineering, 40(7), pp.2085-2093.

[25]. Valenzuela-Jáuregui, J., Ramírez-Bon, R., Mendoza-Galván, A. and Sotelo-Lerma, M. (2003). Optical properties of PbS thin films chemically deposited at different temperatures. Thin Solid Films, 441(1-2), pp.104-110.

[26]. Pentia, E., Pintilie, L., Matei, I. and Pintilie, I. (2001). Field Effect Controlled Photoresistors Based on Chemically Deposited PbS Films. MRS Proceedings, 692.Kumar, S., Sharma, T., Zulfequar, M. and Husain, M. (2003). Characterization of vacuum evaporated PbS thin films. Physica B: Condensed Matter, 325, pp.8-16.

[27]. Kumar, S., Sharma, T., Zulfequar, M. and Husain, M. (2003). Characterization of vacuum evaporated PbS thin films. Physica B: Condensed Matter, 325, pp.8-16.

[28]. Devi, R., Purkayastha, P., Kalita, P. and Sarma, B. (2007). Synthesis of nanocrystallineCdS thin films in PVA matrix. Bulletin of Materials Science, 30(2), pp.123-128.

[29]. Guo, R., Liang, Y., Gao, X., Zhu, H., Zhang, S. and Liu, H. (2014). Microstructure and Near Infrared Absorption of PbS Films Deposited by Chemical Bath Deposition on p-Type Si(100) Wafers. Brazilian Journal of Physics, 44(6), pp.697-702.

[30]. Soetedjo, H., Aziz,, B., Aziz, I., Sudjatmoko, S., 2017. Low resistivity of Cu and Fe doped PbS thin films prepared using dc sputtering technique,. Journal of Non-Oxide Glasses, 9, pp.55–63.

[31]. Bhowmik, R.N., NrisimhaMurty, M. and SekharSrinadhu, E. (2008) 'Magnetic modulation inmechanical alloyed Cr1.4Fe0.6O3 oxide' PMC Physics B, Vol. 1, pp.20–38.

[32]. Hussain, A., Begum, A., Rahman, A., 2012. Characterization of Nanocrystalline Lead Sulphide Thin Films Prepared by Chemical Bath Deposition Technique. Arabian Journal for Science and Engineering, 38(1), pp.169-174.

[33]. Rajathi, S., Kirubavathi, K., Selvaraju, K., 2017. Structural, morphological, optical, and photoluminescence properties of nanocrystallinePbS thin films grown by chemical bath deposition. Arabian Journal of Chemistry, 10(8), pp.1167-1174.

[34]. Fouda, A., Marzook, M., Abd El-Khalek, H., Ahmed, S., Eid, E., El Basaty, A., 2016. Structural and Optical Characterization of Chemically Deposited PbS Thin Films. Silicon, 9(6), pp.809-816.

[35]. KıyakYıldırım, A., Altıokka, B., 2018. Some Physical Properties of The PbS Films Obtained By Chemical Bath Deposition Using Different Molarity Pb(NO3)2 Solution. Dicle University Institute of Natural and Applied Science Journal, 7(1).

[36]. Kole, A., Kumbhakar, P., 2012. Cubic-to-hexagonal phase transition and optical properties of chemically synthesized ZnS nanocrystals. Results in Physics, 2, pp.150-155.